https://doi.org/10.48048/tis.2022.6217

Experimental Investigation of Exterior Reinforced Concrete Beam-Column Connections Subjected to Reversal Loading

Arnon Wongkaew

Department of Civil Engineering, Faculty of Engineering, Burapha University, Chon Buri 20131, Thailand

(Corresponding author's e-mail: arnonw@eng.buu.ac.th)

Received: 22 April 2021, Revised: 29 June 2021, Accepted: 6 July 2021

Abstract

Eight full-scale reinforced concrete beam-column subassemblages, 4 for each non-ductile and ductile detail, were tested under quasi-static cyclic loading. All test specimens were mainly designed for gravity service loads. Four specimens named as non-ductile connections were constructed with typical reinforcement details using in Thailand. The others were assembled with details described by the seismic design building code of Thailand, known as the 1301/1302-61 code. Their performance was examined in terms of lateral load resistance, ductility index, stiffness, energy dissipation, failure modes, including joint shear strength. The test results indicated that the specimens with ductile details achieved better seismic performance in every aspect, particularly specimens with adequate joint shear strength designed according to the SST method. The ductile details have no effect to retard the stiffness degradation in the elastic range, but helped to slow the rates of stiffness degradation after the specimens reached their peak loads. The transverse reinforcement in the joints was more efficient to enhance the ductility of joints with lower joint shear strengths (J1 and J2) than the sufficient joints (J3 and J4). Based on the SST method, the connections with low shear strength capacity, J1, J1D, J2, J2D, J3, and J4 suffered with severe joint shear failure (JS), although their beam sections reached the flexural moments. On the other hand, specimens with high joint shear strengths, J3D and J4D, experienced the beam failure (BF) with mild joint shear failure (JS). Test data also demonstrated that a specimen with lesser amount of joint reinforcement exhibited satisfactory seismic behavior, as long as the joint was provided with the adequate shear strength designed by the SST method. Finally, the ACI 318 Building Code overestimated the shear strength of exterior beam-column joints. Moreover, the simplified SST model much better predicted the demand joint shear strength than the ACI 318 Code.

Keywords: Reinforced concrete, Exterior beam-column joint, Ductile, Transverse reinforcement, Shear, SST method

Introduction

Even though Thailand is not located in a high risk and active seismic zone, the Northern, Western, and some Southern regions of Thailand have a number of active seismic faults passing through the regions. These active faults are capable of generating small to medium earthquakes. As recorded in recent years, there are several medium earthquakes causing damage to buildings located in and nearby the ground motion areas. The seismic activities could even be detected in many tall buildings in Bangkok, but no structural damage was reported. Therefore, Department of Public Works and Town and Country Planning, Thailand, had issued a seismic building code as a guideline for engineers to design structures constructed in these particular zones. The current building code for designing such buildings to resist earthquakes is available to public known as the 1301/1302-61 Code [1]. This building code was developed mainly by adopting seismic design recommendations from many building codes, including the ACI 318 Building Code [2].

Beam-column joints are generally recognized as the critical and vulnerable zone of a reinforced concrete (RC) moment resisting frame subjected to seismic loads [3,4]. Many studies reported that the non-ductile behavior of RC joints caused by the poor detailing of steel reinforcement in the joint area and its surrounding [5,6]. Numerous surveys of RC buildings after earthquakes also confirmed the inadequate detailing of beam-column joints such as presence of splices, lack of hoops, deficiency of beam bar

anchorage, and no steel joint stirrups in the joint. These lead to brittle failure modes in beam-column joints by either the joint shear failure or anchorage slip of beam longitudinal bars, resulting to poorly behave of the RC buildings in the global aspect [7,8]. A significant amount of researches on the seismic performance of RC buildings beam-column joints has been carried out in the last 4 decades. The majority of research literatures has emphasized on improvement of the performance of these RC building beam-column joints through new design concepts and improved details such as the steel joint stirrup and beam anchorage [9-12].

Beres *et al*. [13,14] reviewed through manuals and design codes from the past 5 decades and identified 7 details as typical and potentially critical to safety of gravity load designed building in an earthquake. Their experimental program included testing of 20 interior and 14 exterior full-scale beam-column joints under cyclic static loading. An increase in column axial load resulted in an increase in peak strength for both interior and exterior joints by 15 - 25 %, while it also reduced strength degradation in exterior specimens. Aycardi *et al*. [15] and Bracci *et al*. [16] concluded that the gravity load designed interior and exterior beam-column connections dominantly showed a weak column-strong beam failure. Two exterior joints designed according to pre-1970s practice in New Zealand were tested by Hakuto *et al*. [17]. The joints with negligible transverse reinforcement showed beam hinges when the hooks of beam bars were bent into joint cores. While the joints failed in shear when the hooks were bent out of the joint core. Liu [18] identified the deficiencies of joints were mainly caused by inadequate transverse reinforcement and insufficient anchorage capacity in the joint. A large anchorage length of the beam bars extended into the joints was need to avoid bond failure especial in case of exterior joints. Tran [19] staged that there are 5 key parameters for the joint shear strength included 1) the concrete compressive strength, 2) the vertical joint shear reinforcement, 3) the beam bars detail index, 4) the horizontal joint shear reinforcement and 5) the column axial stress. Among the influence factors, the concrete compressive strength had the most significant correlation to the joint shear strength. Joh *et al*. [20] demonstrated heavy joint shear reinforcement may reduce the slippage of beam bars in the joint and increase the joint stiffness after cracking.

Kaminura *et al*. [21] indicated that the amount of shear reinforcement in the joint had little influence on the strength and deformation of interior beam-column connections. Aavi-Dehkordi *et al*. [22] showed that the failure mode, energy dissipation capacity, pitching behavior, and stiffness of joints with high strength steel bars were similar to those with nominal steel bars. Kang *et al*. [23] reported that the joints with high strength steel bars and concrete exhibited excellent lateral deformation capacity.

A softened strut-and-tie (SST) model was first proposed by Hwang *et al*. [24] to evaluate the shear strength of beam-column joints. The results showed excellent correlation of the joint shear strength predicted by the SST model to available test results. Hwang *et al*. [25] experimentally studied 9-exterior beam-column connections. The shear strength of joints was designed by utilizing the simplified SST model. The study reported that the ACI requirement for joint hoop ratios could be reduced in the exterior beam-column connections. Later, Hwang *et al*. [26] further simplified the SST model, referred to as the "geometric approximation model", for shear prediction of discontinuity regions to facilitate the design practice. The lately proposed method was confirmed to have an accuracy similar to the original SST model.

Since RC buildings are also a common structure in Thailand along with the local practice in RC building construction, it becomes interesting to study the performance of those RC joints in Thailand as well. Therefore, the objective of this study was to evaluate the seismic performance of exterior joints in the existing RC building constructed in Thailand under the gravity service load with the typical joint details. The second objective was to investigate the effect of transverse reinforcement in the joints using the details guided by the building code, 1301/1302-6. The last objective was to evaluate the shear strength of beam-column connections determined from the building code and the simplified SST method. Eight exterior beam-to-column subassemblages were tested under reverse cyclic loading to achieve these objectives. The performance of RC joints reported in terms of their lateral load resistance, ductility, stiffness, energy dissipation, failure modes, including joint shear strength.

Research significance

This study is intended to elaborate the effect of stirrups in the beam-column joint area of exterior RC connections under the large cyclic load. An attempt was made to demonstrate whether the additional stirrups in the joint region could improve overall the seismic performance of connections or not if the joints were provided with adequate shear strength. Also, one of the main parameters to evaluate the seismic performance of connections is the strength-resisting behavior. Hence, the shear strength of joints

provided by the seismic building code of Thailand, 1301/1302-61 [1], ACI 318 [2], and simplified softened strut-and-tie (SST) method [26] were analyzed and compared. As mentioned, the design criteria for RC structures in the 1301/1302-61 Code was adopted from the ACI 318 Building Code. Therefore, to satisfy the standard, the parameters used further in this study were referred as specified by the ACI Code.

Joint shear strength

ACI code method

There are 4 major requirements for the seismic design of beam-column joints specified in the ACI 318 Code [2]. First, the ratio of flexural strengths of columns to beams ($\Sigma M_c/\Sigma M_b$) must be more than 6/5 to satisfy the strong column weak beam design philosophy. Second, the hook bar anchorage development length (l_{dh}) of the beam bar shall not be less than the largest of $8d_b$ (diameter of the beam bar) or 150 mm. Third, the required minimum ratio of the confining reinforcement (ρ_h^{ACI}) for rectangular sections given by Eq. (1) should be satisfied;

$$\rho_h^{ACI} = 0.3\frac{f_c^{'}}{f_{yh}} = \left(\frac{A_g}{A_{ch}} - 1\right) \text{ and not less than } 0.09\frac{f_c^{'}}{f_{yh}} \quad (1)$$

where f_{yh} is the yield strength of the hoop reinforcement; A_g is the gross column section area; and A_{ch} is the section area of column core measured out-to-out of hoop reinforcement.

Finally, the design shear forces acting on joints (V_{ju}^{cal}) shall not exceed the nominal joint shear strengths ($\emptyset V_{jn}^{ACI}$), which is classified according to geometry and confinement of the joints (Eq.(2)). The details of those requirements can be found in the ACI Code. The nominal joint shear strength given in the 1301/1302-61 [1] and ACI Code is calculated by;

$$V_{ju}^{cal} \leq \emptyset V_{jn}^{ACI} = 0.85(\gamma\sqrt{f_c^{'}}A_j) \quad (2)$$

where γ is equal to 1.7, 1.25, or 1.0, depending on the geometry and the level of the confinement exerted by the beams. For this study, the γ value of 1.0 was taken for the exterior connection. $f_c^{'}$ is the concrete compressive strength. A_j is the effective joint area to resist the transferred shear force as shown in **Figure 1(a)**, and shear resistance factor ($\emptyset$) is 0.85. For the exterior joint shown in **Figure 1(b)**, the horizontal shear (V_{ju}^{cal}) at the midheight of the joint is estimated as;

$$V_{ju}^{cal} = T_n - V_{col}^{cal} \quad \text{or} \quad V_{ju}^{test} = T_n - V_{col}^{test} \quad (3)$$

where the joint shear (V_{ju}^{cal}) and (V_{ju}^{test}) are equal to the nominal force in the top steel acting to the joint assuming a beam section reaching its nominal flexural capacity (M_{nb}), minus the shear in the column due to sway of the column. The column shear (V_{col}^{cal} *and* V_{col}^{test}) can be obtained from a frame analysis. For most practical cases, they are estimated from the free-body diagram in **Figure 1(c)**, where points of contraflexure are assumed at the midheight of each story, similar to the experimental setup in this study. The only difference between V_{col}^{cal} and V_{col}^{test} is the first 1 determined from equilibriums of the joint with assumed M_{nb} at the face of column and the other with the applied peak load, P_{max} from the test. The force T_n is the tension of the reinforcement in the beam at its nominal capacity as;

$$T_n = \alpha A_s f_y \quad (4)$$

The factor α is intended to account for the fact that the actual yield strength of beam bars is larger than the specified strength. The high probability that those bars can go into strain hardening if plastic hinges form in the beams adjacent to the column faces. The value of 1.25 was suggested [2] and adopted for this study.

Softened strut-and-tie (SST) method

Since the current ACI provisions emphasize the importance of confinement in the joint core, this usually leads to close spaced transverse reinforcement in the region. These requirements make the congested reinforcement in the joint, and are very difficult to construct. Moreover, the recent test results indicated fewer joint stirrups with wider spacing can be used without significantly affecting the performance of connections if the joints have the adequate shear strength [25]. One of the best models to

predict the shear strength of the RC connections is a softened strut-and-tie (SST) model, proposed in 1999 by Hwang *et al*. [24], and had been simplified lately in 2017 [26]. In this SST model, the required amount and spacing limits of the joint hoops suggested by the ACI Code [2] can be reduced. For this study, the simplified SST model was adopted to evaluate the shear strength of the joints. As shown in **Figure 1(d)**, the joint shear is transferred by the strut-and-tie model through the diagonal compression strut (C_d) with an inclined angle of θ. Based on the simplified version of the SST model, the nominal horizontal shear strength of joints can be defined as;

$$\emptyset V_{jn}^{SST} = 0.85 C_{d,n} cos\theta = 0.85 K \xi f_c^{'} A_{str} cos\theta \quad (5)$$

where $C_{d,n}$ is the nominal diagonal compressive strength of the joint. θ is the angle of inclination between diagonal strut and the horizontal axis. K denotes the strut-and-tie index. ξ represents the softening coefficient of cracked reinforce concrete. $f_c^{'}$ indicates the compressive strength of a standard concrete cylinder. A_{str} defines the effective area on the nodal zone of the diagonal strut. The shear resistance factor ($\emptyset$) is 0.85, similar as given by the ACI Code. The complete set of the design equations and procedures are available in ref. [26].

Experimental program

Specimen and material properties

Eight full-scale specimens of exterior RC beam-column joints were tested in this study. The column height (H) was kept constant at 2,725 mm with the beam lengths (L_b) as shown in **Table 1**. Since the column depths were varied, while the distance between the center of actuator to the support was constant, resulting in the different beam lengths (L_b) of those specimens. Four specimens were constructed with typical steel reinforcement detailing for RC buildings constructed in Thailand, named as non-ductile details, J1 - J4. The others were conducted with steel reinforcement detailing described by the building code, 1301/1302-61 [1], known as ductile details, J1D - J4D. **Figures 2(b) - 2(e)** presented the reinforcement details for non-ductile and ductile test RC connections. As can be seen, the differences between these 2 groups were 1) spacing of stirrup reinforcement arranged more closely in the beam and column regions near the joints, and 2) the additional stirrup assigned into the column joints. It should be noted that approximate 25 % of minimum transverse reinforcement required by the ACI code [2] were applied. This reduction conformed to the previous study [25] stated that this reinforcement could be relaxed as long as the joint provides the sufficient shear strength to resist the shear demand. The beam and column cross-section sizes, proportion and reinforcement amounts, and details of the specimens were obtained from the as-built drawing of a typical 5-story RC building constructed without seismic consideration in Thailand. The ratios of the flexural strength of columns to beams ($\Sigma M_c/\Sigma M_b$) and the hook bar anchorage development lengths (l_{dh}) for all test specimens fulfilled the minimum requirements of the ACI 318. However, the required minimum ratios of the confining reinforcement (ρ_h^{ACI}) did not meet the minimum requirement as mentioned above. All test specimens were designed with sufficient shear strengths varied from 29 - 53 % over the demand shear forces calculated from the ACI 318 by Eq. (2). On the other hand, from the perspective of the SST model, Eq. (5), the shear strength of joints J1, J1D, J2, J2D, and J4 were deficient by 14 - 89 % from their demand as shown in **Table 1**. The test-day compressive strength obtained from average values of 3 150×300 concrete cylinders for each specimen was also reported. **Table 1** presents geometries, structural indices, the ACI Code requirements, and joint shear strength ratio of the test specimens.

Table 1 Geometrical, structural indices, ACI requirements, and joint shear strength ratio of the test specimens.

Name	Column	Beam	L_b (mm)	$f_c^{'}$ (MPa)	M_n^c (kN-m)	M_n^b (kN-m)	ACI requirements			Estimated joint shear strength ratio	
							$\frac{M_n^c}{M_n^b}$	l_{dh} (mm)	$\frac{\rho_h}{\rho_h^{ACI}}$	$\frac{V_{ju}^{cal}}{\emptyset V_{jn}^{ACI}}$	$\frac{V_{ju}^{cal}}{\emptyset V_{jn}^{SST}}$
J1	250×250	200×400	2,395	31.3	92.4	55.6	1.66	212	-	0.60	1.89
J1D				28.0	91.3	55.2	1.65	224	0.25	0.64	1.63
J2	270×300	270×400	2,345	31.3	117.4	82.8	1.42	212	-	0.70	1.76
J2D				30.0	117.0	82.6	1.42	216	0.28	0.71	1.55
J3	300×400	220×400	2,245	31.3	115.4	81.8	1.41	212	-	0.47	0.93
J3D				30.0	115.0	81.6	1.41	216	0.25	0.48	0.87
J4	250×400	250×400	2,245	31.3	324.0	82.4	3.93	212	-	0.56	1.14
J4D				30.0	322.0	82.2	3.92	216	0.23	0.58	1.04

H = 2,725 mm, "-" no horizontal reinforcement in the joint area

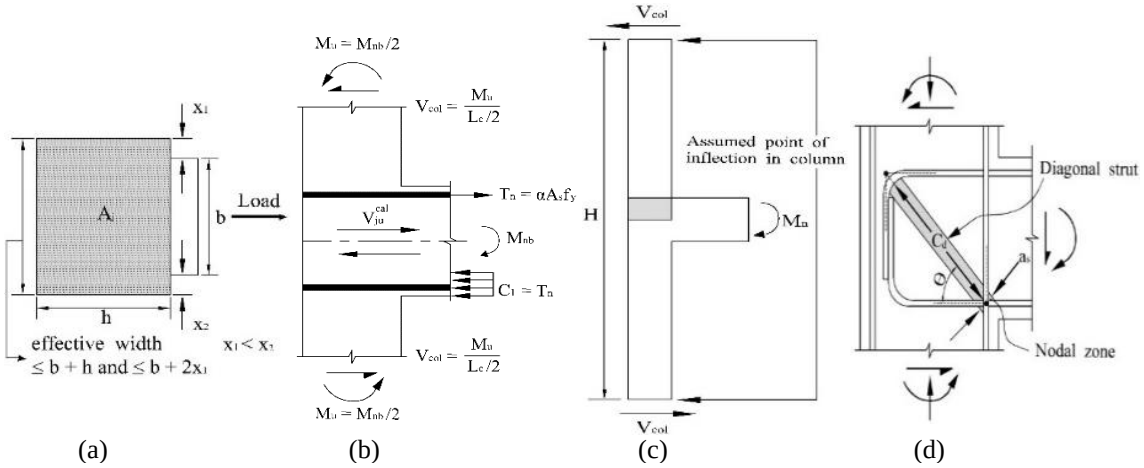

Figure 1 (a) Effective area (Aj) of the typical exterior connection [1]; (b) Shear force transfer mechanism in the typical exterior connection [5]; (c) Free-body diagram of the typical exterior connection when the beam reaches its nominal flexural capacity; (d) Diagonal strut mechanism [24].

Figures 2(b) - 2(e) depicted a drawing of the dimensions and reinforcement details for the test units, group 1 - 4. The main reinforcement for beams and columns were 16 mm diameter deformed bars (DB), except group 4 columns of 20 mm diameter DB. Each top and bottom main beam reinforcement ended with a 90 ° hook bend into the joint with an extension of the depth of beams. Since all beam depths were 400 mm, the hook bar anchorage development lengths (l_{dh}) as shown in **Table 1** satisfied the requirement. The size of stirrups in beams and columns were 6 mm diameter round bars (RB). Also, the stirrups were extended through the column joints for the ductile details as specified in **Figure 2(a)**. On the other hand, the stirrups of non-ductile specimens were stopped at the level of top and bottom beam depths. Also the standard 135 ° hooks at the ends of stirrup bars were applied. The concrete cover of 30 mm was assigned for all cross sections. The average test yield and tensile strengths of steel bars were given in **Table 2**.

Table 2 Material properties of steel.

Reinforcing bar	Yield strength (MPa)	Ultimate strength (MPa)
DB20	520	620
DB16	400	580
RB6	365	560

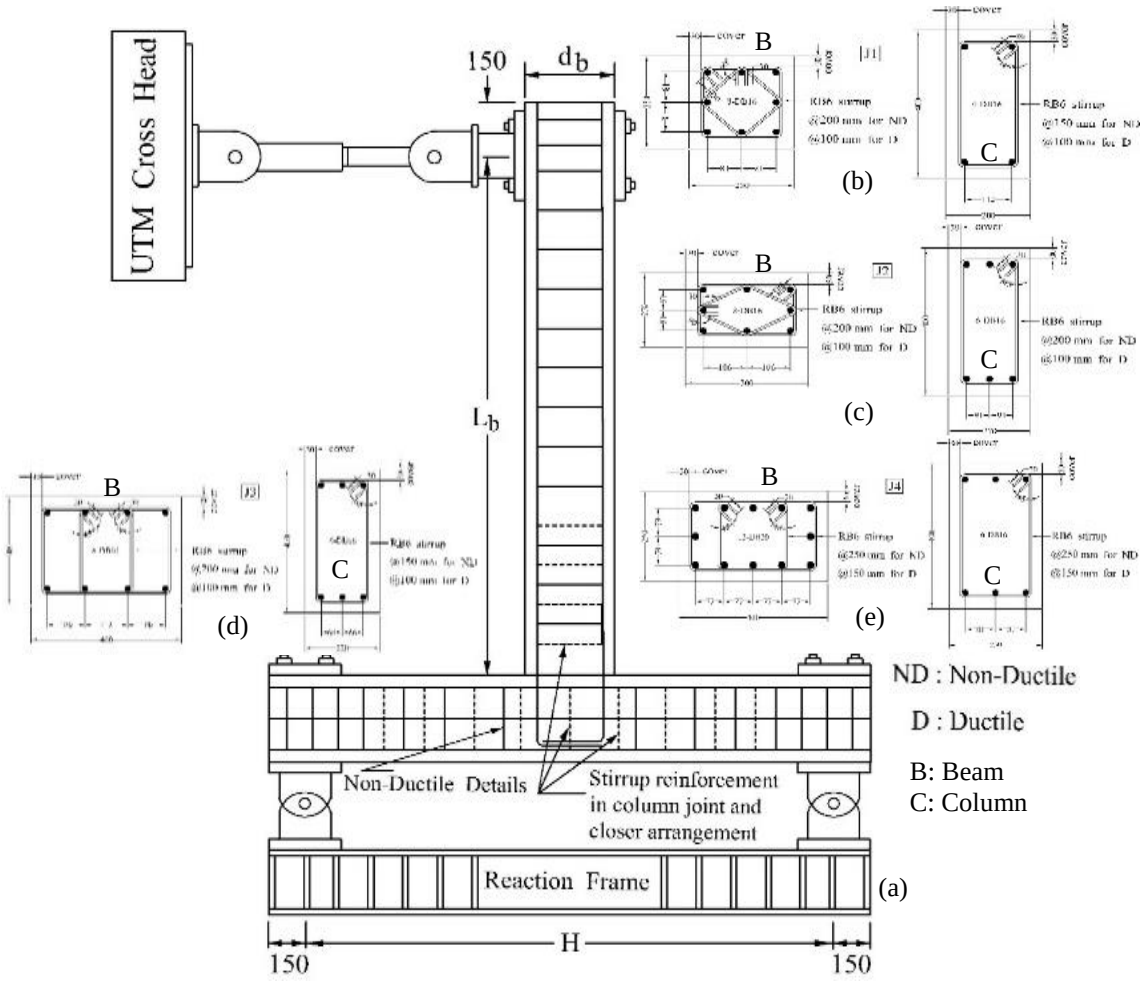

Figure 2 Schematic of non-ductile (ND) and ductile details (D) of the test RC beam-column joints.

Test setup, load history, and instrumentation

A schematic view of the test setup and boundary conditions is illustrated in **Figures 3(a) - 3(b)**. The figure represents an exterior joint subassemblage from the typical RC moment resisting frames. The subassemblage was made by considering that the moment at the mid-height of a story and the mid-span of a beam were generally close to 0 under the typical seismic loading allowing an assumption of the pin boundary condition at those points, as shown. Therefore, the column was mounted vertically with pinned supports at the both ends. The lateral cyclic load was applied at the end of the beam through a hinge joint attached to a 1,500 kN universal testing machine (UTM). It should be noted that UTM and steel reaction wall were mounted to the 2 m thick strong floor. This experimental setup represented an out-of-frame applied loading to an assembly of the beam-column joint specimen by utilizing the UTM as a hydraulic actuator. The sketch and photograph of this test setup was also illustrated in **Figures 3(c) - 3(d)**. The loading protocol was a quasi-static cyclic displacement pattern as defined by the ACIT1.1-01 [27] with the input rate of 1 mm/1 min. The displacement history was also in **Figure 3(e)**. Each story drift consisted of 3 cycles of push down and pull up. The displacement loading was applied to each specimen until either fracture occurred, resulting in a significant loss of strength, or a story drift of 5 % radians was reached. Each specimen was carefully instrumented to measure rotation, displacement, and strain of particular parts of the joint such as the top and bottom of beam near the joint. The column, beam, and joint deformation were measured using 18 Linear Variable Differential Transducer (LVDT) as shown. The total applied displacement was measured by the actuator LVDT of UTM. Two LVDT were also installed at the level of the actuator head to verify the displacement reading from UTM.

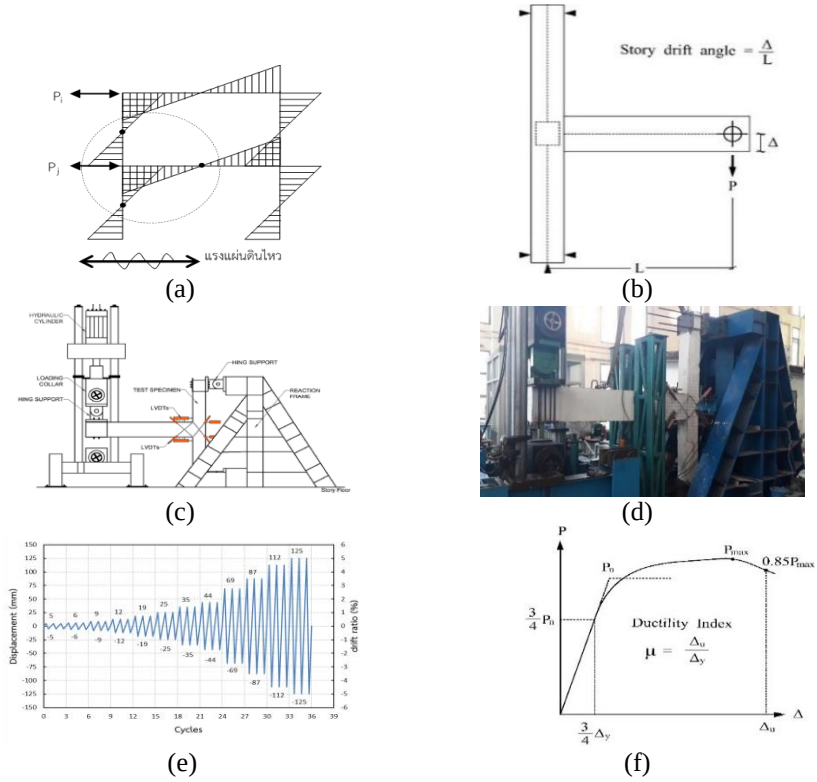

Figure 3 Test setup, boundary condition, quasi-static cyclic displacement pattern (e) [27].

Results and discussion

Hysteretic, peak loads responses, and ductility

Hysteretic and their corresponding peak-loads responses of all test specimens were displayed in **Figures 4(a)** - **4(h)**. Ultimate load, stiffness, energy dissipation, and ductility index were summarized in **Table 3**. The results were presented by comparing between pairs of the non-ductile and ductile joints as described previously. As shown, the maximum loads in the positive (downward) direction occurred at a same drift ratio of 3 % for both specimens with values of 35 and 40 kN for J1 and J1D, respectively. In the negative (upward) direction, the maximum load of J1 occurred at 3 % drift with a value of −28 kN. However, J1D had the maximum load at 2.75 % drift with a value of −32 kN. Therefore, the average ratio between the peak loads in both directions of each specimen was equal to 1.25, which showed that the downward has more resistance capacity than the upward direction around 25 %. This indicated that J1 and J1D suffered from the bond slip of the bottom beam bars earlier than the top bars. Although the bond slip of J1D occurred prior to J1, the resistance strength of the joint in the downward direction was still maintained at this level then slowly decreasing rather than suddenly drop as presented by J1. The maximum load of J2 occurred at 2 % drift with a value of ± 32 kN in both directions and maintained the resistance strength to 2.75 % drift. This specimen also demonstrated the bond slip of the beam bars. For J2D, the maximum loads occurred at 3.75 % drift with a value of 39 kN in positive (downward) direction, and −47 kN at 3 % drift in the negative (upward) direction. The ratio between the peak loads in both directions of J2 is equal to 1.0. In the meantime, J2D has a value ratio of 1.21. Opposite to group 1, the bond slip of the top beam bars occurred when the load was applied downward resulted to the lower load resistance. Overall behavior of the ductile joint, J2D, obviously demonstrated the better behavior in terms of peak loads and their corresponding drift displacements. The maximum loads of J2D was about 22 and 47 % higher than J2 in the positive and negative directions, respectively. Moreover, the joint J2D sustained at the peak load level longer than J2, with slowly dropped off its strength, as shown in **Figure 4(d)**. Specimen J3D clearly revealed the better hysteretic behavior comparing to J3. The maximum load of J3D had a value of ± 62 kN in both load directions, but differently occurred at 3.5 and 4.75 % drift in the positive and negative directions, accordingly. Similarly, J3 had the peak loads with a value of about ± 50 kN in both load directions. This pair of specimens indicates no bond slip of the beam bars occurred in the joints. As mentioned, J3D has the maximum load about 24 % higher as well as better retaining the

maximum load than J3. The pair of specimens, J4 and J4D, showed similar behavior comparing to the others. The maximum loads of the ductile joint, J4D, was slightly higher by 5 and 10 % in the positive and negative directions. The bond slip of the beam bars was detected from J4 as well. Importantly to point that specimens, J3, J3D, and J4D have the shear strength capacity of the joints more than their demands by 14, 26 and 4 % with respect to the SST method, resulting in no bond slip of the beam bars. Failure modes of test specimens will be discussed later.

The seismic responses of specimens in group 1 and 4 were almost similar, regardless of their ductile details. Perhaps, it was resulted from the moment capacity of columns were designed much higher than of beams. On the other hand, the specimens in group 2 and 3 with the ductile details, J2D and J3D, displayed much better seismic behavior, particularly after the maximum loads. The specimens can sustain the peak loads up to 4 % drift with disregard of their failure. The other observation from the test was on specimen J3D. Unlike others, this specimen demonstrated a remarkable seismic performance in all aspects; strength, ductility, energy dissipation, and failure mode. According to simplified SST [26], these behavior might contribute to the inclination angle θ of the diagonal compressive strut in the joint area, and to the effective area on the nodal zone of the diagonal strut (A_{str}) to resist the transferred shear force. When the angle θ is approached 45 degrees, the main diagonal strut resists most of the force in the D-region area. As can be seen from **Table 4**, specimen J3D has the angle θ of 46 degrees and A_{str} of 30,000 mm^2, maximum values among specimens. Also, it should be noted that the transverse reinforcement of this specimen was only 25 % of minimum requirement from the ACI Code, but the specimen has enough joint shear strength according to the SST method. Therefore, this indicates that the stirrup reinforcement in joint areas still plays the important role to restrain strength and stiffness degradation of the connections after the peak load. However, relaxation on transverse reinforcement of the joints may be applied to the ACI Code [2].

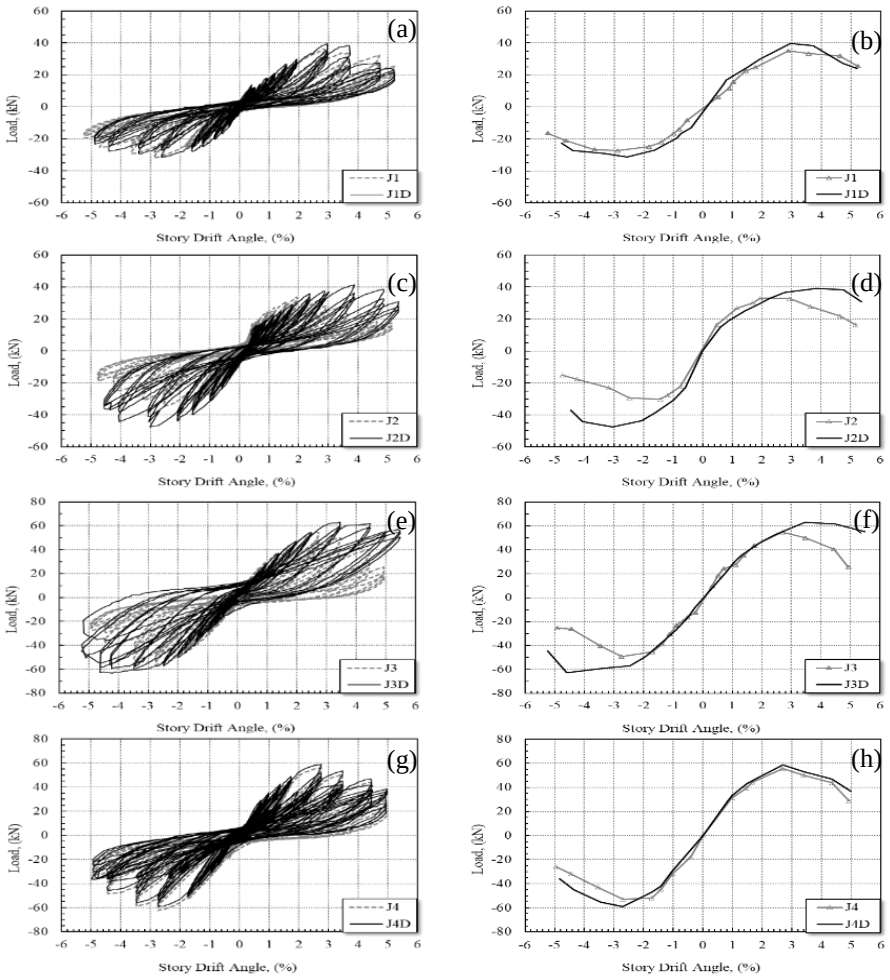

Figure 4 Hysteretic response and envelope of hysteretic loops of test specimens.

The ultimate load, maximum stiffness, energy dissipation, and ductility index were summarized in **Table 3**. All specimens reached their flexural moment capacity of beams as show in the table. The displacement ductility index is defined as Δ_u/Δ_y, as shown in **Figure 3(f)**. Where Δ_u is the vertical displacement measured at the beam tip corresponding to ultimate load (P_u), defined at 15 % reduction of the maximum load (P_{max}). The yield displacements, Δ_y, for all test specimens were determined by extrapolating the displacement at $0.75M_n$, linearly to M_n, which is the nominal flexural strength of the beams. As shown, all specimens with the ductile details returned on higher displacement ductility index by about 13 to 141 %. However, the transverse reinforcement in the joints was more efficient to enhance the ductility of joints with lower shear strengths (J1 and J2) than joints with sufficient shear strengths (J3 and J4), according to the SST method.

Stiffness degradation

Peak-to-peak stiffness method was employed to access the behavior of specimens tested under quasi-static loading in terms of the reduction of lateral stiffness. The peak-to-peak stiffness values, known as the slope of a straight line drawn from the peak loads reached on both positive and negative directions in each load cycle, were calculated using Eq. (6) [28];

$$K_t = \frac{P_{1,i}+P_{2,i}}{\Delta_{1,i}+\Delta_{2,i}} \quad (6)$$

where $P_{1,i}$, $P_{2,i}$, $\Delta_{1,i}$, and $\Delta_{2,i}$values are peak lateral loads of the positive and negative directions for the third cycle of i^{th} loading sequence and the corresponding drifts, respectively.

The plot of stiffness against the drift angle for all specimens was shown in **Figures 5(a)** - **5(h)**. To investigate the degradation rate, the stiffness of each drift was normalized with respect to the stiffness of the first drift (KI). As seen, the stiffness degradations were approximately categorized into 3 zones as from initial to yielding, yielding to ultimate, and ultimate to failure stages, corresponding to 0 - 1, 1 - 3, and 3 - 5 % drift levels, respectively. In elastic stage, regardless of steel reinforcement details, the lateral stiffness of all joints significantly and rapidly reduced from their initial values between the drift levels of 0.2 - 1 % which were considered loss of lateral resistance at such low drift levels. Although, the initial stiffness of ductile specimens was apparently higher than non-ductile, the ductile joints displayed more stiffness degradation than non-ductile details. It indicated that the additional stirrups in the joints have no effect to retard the stiffness degradation in the elastic range. Then, the stiffness of joints gradually declined when the drift levels progressed to 3 %, where the maximum loads of most specimens were reached, except J2 and J4. Also, there was no clear evidence to show significant modification in stiffness reduction of ductile over non-ductile details for this stage. However, after the specimens reached their peak loads (solid spots in **Figures 5(a)** - **5(h)**), the ductile joints showed lower rates of stiffness degradation, especially specimens of group 2 and 3. The reserved stiffness after peaks of non-ductile and ductile specimens varied between 18 - 29 and 5 - 18 %, respectively. This result was similar to conclusion drawn from other researchers that the additional stirrups in the joints helped to rather delay the joint deterioration than increasing the stiffness of the joints [25].

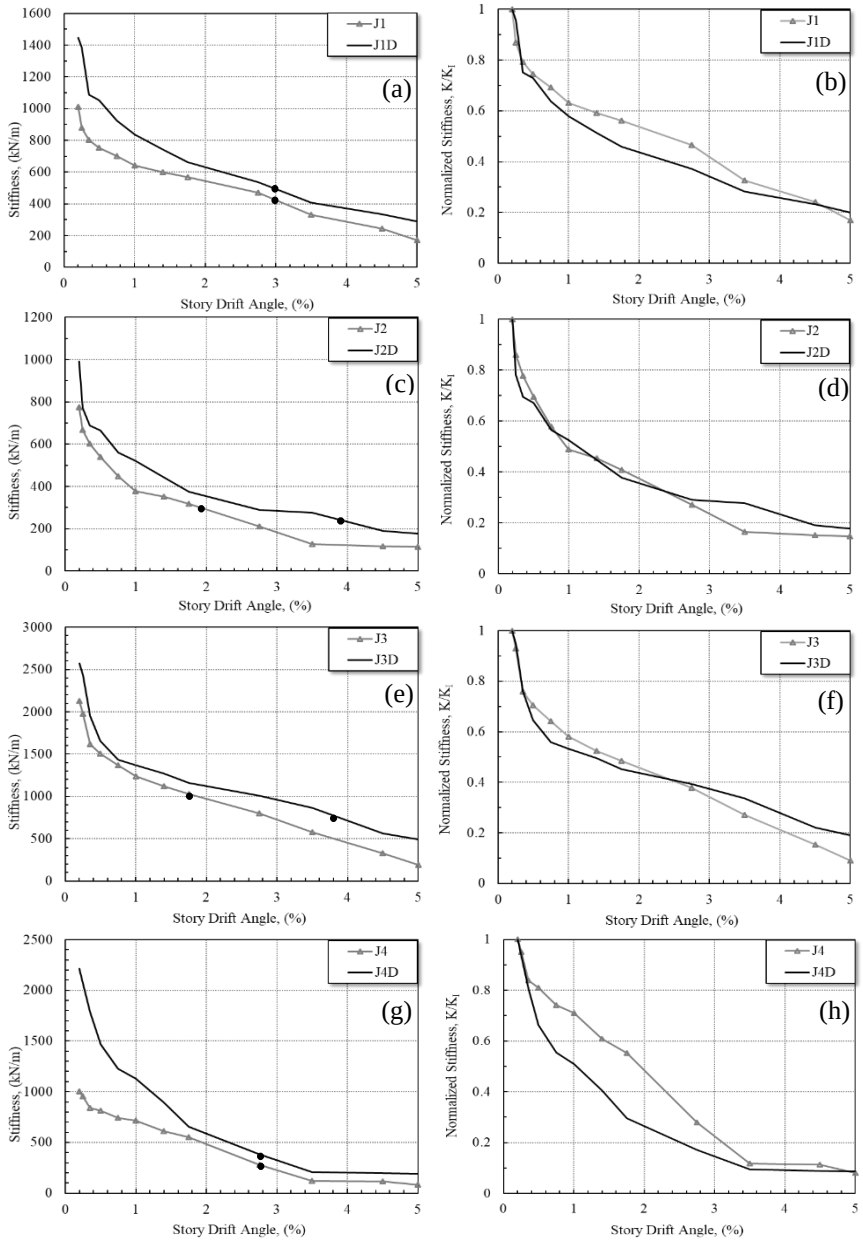

Figure 5 Stiffness degradation of test specimens.

Energy dissipation

The ability of structural element to resist an earthquake load depends on a large extent of its capacity to dissipate energy. Energy dissipation can be calculated from the area enclosed in a plot of load versus displacement for each particular cycle. The comparison of cumulative energy dissipation between 2 specimens of each group was presented in **Figures 6(a)** - **6(d)**. In general, only a small amount of energy was absorbed during the initial several loading steps. As the beam-column specimen was damaged due to the cyclic loading at the higher drift levels, then energy absorption gradually to rapidly increased, depending on pairs of specimens. Overall behavior of cumulative energy dissipation for the ductile specimens was higher than the non-ductile detail. J1 - J1D (a), J2 - J2D (b), J3 - J3D (c), and J4 - J4D (d) had total energy dissipation of 56 - 88, 64 - 88, 70 - 255 and 90 - 112 kN-m, respectively, by the end of each test. Specimen J1 and J1D had almost a same absorption level up to 0.75 % drift, then J1D with ductile details rapidly starting to participate in energy absorption much higher than J1. Total energy of J1D was computed as 32 % higher than J1 by the end of 5 % drift. Specimen J2 - J2D and J4 - J4D demonstrated similar energy participation behavior as slowly involving in absorption up to a drift of 1.75

%, after that the specimens with ductile details gradually engaged in energy over the non-ductile detail, as 38 and 24 % by the end of tests, respectively. Obvious cumulative energy dissipation was occurred with a pair of specimen J3 and J3D. As shown, J3D joint rapidly started to contribute in energy captivation after 0.75 % drift. This J3D joint delivered total energy absorption of 255 kN-m, increasing of 264 % higher than J3, by the end of test at 5 % drift. Thus, the highest increasing of energy absorption was approximately 264 % from J3D and the lowest increment of energy dissipation of 24 % from J4D.

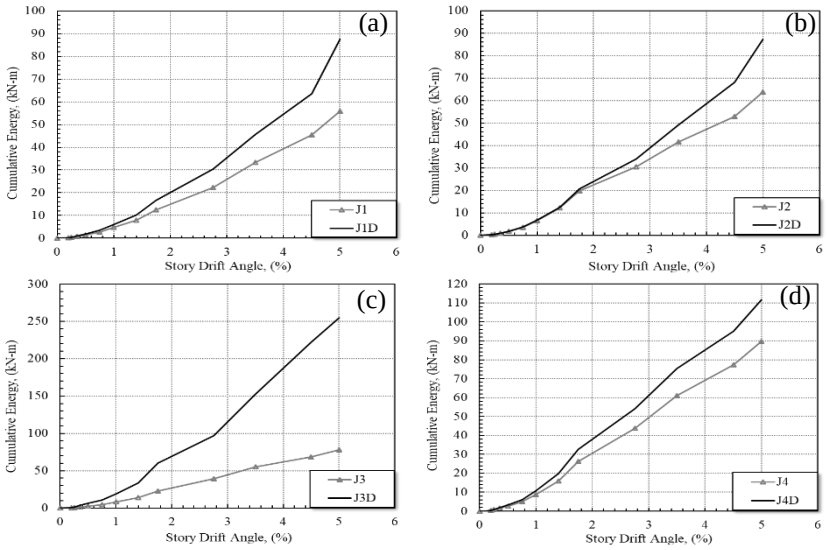

Figure 6 Cumulative energy dissipation of test specimens.

Failure mode

All test specimens had similar damage in the beam, column, and joint regions which were categorized into 2 main types of failure as the joint shear failure (JS) **Figures 7(a)** - **7(d)** or the beam failure (BF) **Figures 7(e)** - **7(h)**. The JS refers to failures due to shear force in the joint area causing the crushing and spalling of column concrete. The BF refers to the beam flexural failures due to bond slip following by the buckling of the beam bars (beam hinging). In addition, the BF-JS refers to the joint shear failure after the beam hinging. Photographs of these 2 different modes of damaged specimens were illustrated in **Figures 7(a)** - **7(h)**. Generally, the first indication of damage in the joint was cracking of the concrete. Initially, cracking occurred at the perimeter of the joint due to flexural loading of the beams. Later on as loading progresses, diagonal cracks occurred within the joint due to shear loading of the joint core. First damage stage (a, e), flexural cracks typically initiated at the tension face of the beam, as well as at the beam-joint interface under the tension force. These cracks were of hairline with immeasurable width. As can be seen, these cracks were generated at the drift levels between approximately 1 - 2 %. Second stage (b, f), cracks propagated vertically further and into the joint from the joint corner under tension. After drift ratio of 2 %, the cracks extended pass through the joint as a diagonal from the beam corner to the column far-end face. Third stage (c, g), additional cracks were concentrated in the joint area at the drift levels of 3 - 4.5 %. Up to this stage, non-ductile and ductile specimens had somewhat similar failure patterns, except minimum cracks occurred with the ductile rather non-ductile details. Fourth stage (d, h), the specimens with the non-ductile details started to loss their resistance strength as those cracks more spreading and widen into the joint area. This stage was identified as level of 4.5 - 5.5 % drifts. On the other hand, even though the ductile specimens show similar cracking patterns with only thinner width, no severe diagonal crack and spalling of concrete in the joint were detected as shown in **Figures 7(d)** - **7(h)**. Failure types of test specimens were concluded in **Table 4**.

Table 3 Ultimate loads, energy dissipation, ductility of specimens.

Results	Group 1		Group 2		Group 3		Group 4	
	J1	**J1D**	**J2**	**J2D**	**J3**	**J3D**	**J4**	**J4D**
Ultimate load (kN)	35 −28	40 −32	32 −32	39 −47	50 −50	62 −62	55 −54	58 −59
(P_n)	(24)	(24)	(32)	(32)	(36)	(36)	(37)	(37)
Max. stiffness (kN/m)	1,013	1,385	773	992	2,131	2,437	1,000	2,214
Energy dissipation (kN-m)	56	88	64	88	78	255	90	112
Avg. ductility index (Δ_u/Δ_y)	3.3	5.0	2.1	5.0	2.8	3.9	3.3	3.8

Positive means downward direction; Negative means upward direction; P_n are computed at the beams reaching their flexural moment capacity.

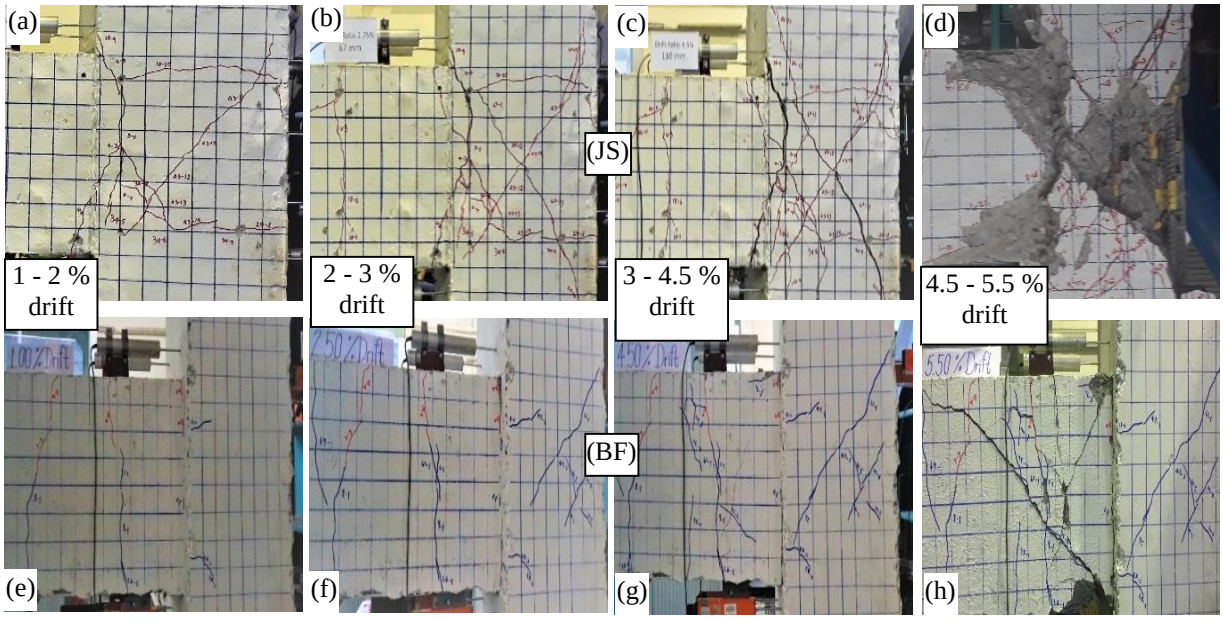

Figure 7 Damage of tested specimens for non-ductile and ductile joints.

Comparison of joint shear strength computed from SST method [26] and ACI Code [2]

As shown in **Tables 1** and **4** the shear strength ratios between the demand capacity computed at the beam yield (V_{ju}^{cal}) and at the maximum test load (V_{ju}^{test}) to the joint shear capacity ($\emptyset V_{jn}^{ACI}$) calculated from the ACI Code were all less than 1. It implied the beam failure (BF) should be the govern failure criteria for all specimens. However, the test results exhibited an opposite failure type of the joint shear failure (JS). Obviously, this result indicated that the ACI 318 overestimated the shear strength of the exterior beam-column joints. On the other hand, the same demand shear strengths were normalized with the joint shear strengths ($\emptyset V_{jn}^{SST}$) determined by the simplified SST model [26]. The results showed that specimens J1, J1D, J2, J2D, and J4 had the joint shear capacity only 56, 65, 57, 67 and 95 % of their shear demands at the maximum loads, respectively. Therefore, the joint shear failure (JS) was obtained with those specimens as expected by the SST model. Furthermore, the shear strength capacity of the joints J3D and J4D, which were 26 and 4 % more than the demand shear strengths exhibited the beam failure (BF). Despite, there was an exception occurred with the specimen J3. The joint shear strength was calculated about 14 % higher than its demand, yet the specimens failed by BF-JS. Regardless of this, it can conclude that the simplified SST model much better predicts the nominal joint shear strength than the ACI 318. As

mentioned earlier, the accurate determination of the joint shear capacity which is critical to seismic performance of beam-column connections can lead to lower of transverse reinforcement in the joint area. Therefore, the further study on this topic is definitely need to verify this current finding.

Table 4 Joint shear strength and failure mode.

Name	A_j (mm^2)	θ (Degree)	A_{str} (mm^2)	K	V_{ju}^{test} (kN)	$\frac{V_{ju}^{test}}{\emptyset V_{jn}^{ACI}}$	$\frac{V_{ju}^{test}}{\emptyset V_{jn}^{SST}}$	Failure Mode
J1	62,500	64	15,625	1	170	0.57	1.79	JS
J1D				1.30	168	0.60	1.53	JS
J2	81,000	57	20,250	1	270	0.70	1.76	JS
J2D				1.19	261	0.69	1.50	JS
J3	120,000	46	30,000	1	252	0.44	0.88	BF - JS
J3D				1.12	245	0.44	0.79	BF
J4	100,000	47	25,000	1	248	0.52	1.05	JS
J4D				1.14	248	0.53	0.96	BF

JS means joint shear failure; BF means flexural failure of beam hinging; and BF - JS means joint shear failure after beam hinging.

Conclusions

An experimental program was conducted to evaluate the seismic performance of exterior RC beam-column joints. Eight test units are the full-scale models of typical exterior joints for the 5-story RC building currently existing in Thailand. Four specimens were considered as non-ductile specimens which were designed with the reinforcement details for the gravity service loads only. The others built with the same column and beam dimensions and primary reinforcement, except adding of transverse reinforcement into the joints and surrounding areas as described by seismic design code of Thailand, 1301/1302-61 [1]. The results from the experiment were compared and analyzed. The findings can be concluded as follows,

1) The test results indicate that the exterior RC joints with ductile details seismically perform better than non-ductile joints in terms of ultimate load, stiffness, energy dissipation, ductility, and failure modes. This indicates the important role of additional stirrup reinforcements in the joint area.

2) The ductile details increased ultimate load by 5 - 24 % in positive and 9 - 47 % in negative directions, approximately.

3) The ductile details have no effect to retard the stiffness degradation in the elastic range, but helped to slow the rates of stiffness degradation after the specimens reached their peak loads. The maximum stiffness of ductile specimens was increased by about 14 - 121 %.

4) Overall behavior of cumulative energy dissipation for the ductile specimens was higher than the non-ductile details varied from 24 % to as much as 227 % for J3D. Also, there was no bond slip of the beam bars occurred in this pair of joints.

5) All specimens with the ductile details returned on higher displacement ductility index by about 13 - 141 %. However, the transverse reinforcement in the joints was more efficient to enhance the ductility of joints with lower joint shear strengths (J1 and J2) than the sufficient joints (J3 and J4).

6) Based on the SST method, the beam-column connections with low shear strength capacity, J1, J1D, J2, J2D, J3 and J4 suffered with severe joint shear failure (JS), although their beam sections reached the flexural moments. On the other hand, specimens with high joint shear strengths, J3D and J4D, experienced the beam failure (BF) with mild joint shear failure (JS).

7) The ACI 318 overestimates the shear strength of the exterior beam-column joints by approximately 44 - 70 %. Moreover, the simplified SST model much better predicts the demand joint shear strength than the ACI 318.

8) The deterioration of beam-column joints under seismic could be effectively restrained by the ductile details according to 1301/1302-61 code with adequate shear strength capacity determined by using the equation of SST model.

Acknowledgements

Authors would like to thank all recent and former students, including technician staffs of Department of Civil Engineering, Burapha University, Thailand who made contribution in anyways to this study. Also, sincerely thank would be extended to National Research Council of Thailand for grant supports (2560A10802186 and 256109A1080017), and a grant from Engineering School, Burapha University, Thailand (contract no. 61/2552).

References

[1] Department of Public Works and Town and Country Planning. *Standard building design code for buildings resisting earthquakes (1301/132-61)*. S. P. M. Printing, Bangkok, Thailand, 2018.
[2] American Concrete Institute Committee. *ACI CODE-318-19: Building code requirements for structural concrete and commentary*. American Concrete Institute, Michigan, 2019.
[3] DT Thinh. 2003, Seismic performance of reinforced concrete beam-column subassemblages without seismic detailing. Ph. D. Dissertation. Asian Institute of Technology, Bangkok, Thailand.
[4] PC Pantelides, J Hansen, J Nadauld and LD Reaveley. *Assessment of reinforced concrete building exterior joints with substandard details*, Pacific Earthquake Engineering Research Center, College of Engineering, University of California, Berkeley, 2002.
[5] T Paulay and MJN Priestley. *Seismic design of reinforced concrete and masonry buildings*. John-Wiley & Sons, New Jersey, 1992.
[6] T Paulay and R Park. *Joints of reinforced concrete frames designed for earthquake resistance*. National Library, Christchurch, New Zealand, 1984.
[7] C Cheejaroen. 2004, Effect of bond deterioration on seismic of R/C interior beam-column joint without seismic detailing. Ph. D. Dissertation. Asian Institute of Technology, Bangkok, Thailand.
[8] CKR Siva and GS Thirugnanam. Comparative study on behavior of reinforced beam-column joints with reference to anchorage detailing. *J. Civ. Eng. Res.* 2012; **2**, 12-7.
[9] F Alemdar and H Sezen. Shear behavior of exterior reinforced concrete beam-column joints. *Struct. Eng. Mech.* 2010; **35**, 123-6.
[10] A Sharmaa, GR Reddya, R Eligehausenb and KK Vazea. Strength and ductility of RC beam-column joints of non-safety related structures and recommendations by national standards. *Nucl. Eng. Des.* 2011; **241**, 1360-70.
[11] IS Misir and S Kahraman. Strengthening of non-seismically detailed reinforced concrete beam-column joints using sifcon blocks. *Sadhana* 2013; **38**, 69-88.
[12] MTD Risi and GM Verderame. Experimental assessment and numerical modelling of exterior non-conforming beam-column joint with plain bars. *Eng. Struct*. 2017; **150**, 115-34.
[13] A Beres, SP Pessiki, RN White and P Gergely. Seismic performance of existing reinforced concrete frames designed primarily for gravity loads. *In*: Proceedings of the 16th Canadian Conference on Earthquake Engineering, Ontario, Canada. 1991, p. 655-62.
[14] A Beres, RN White, P Gergely, SP Pessiki and A El-Attar. Behavior of existing non-seismically detailed reinforced concrete frames. *In*: Proceedings of the Tenth World Conference on Earthquake Engineering, Balkema, Rotterdam. 1992, p. 3359-63.
[15] LE Aycardi, JB Mander and AM Reinhorn. Seismic resistance of reinforced concrete frame structures designed only for gravity loads: Experimental performance of subassemblages. *ACI Struct. J*. 1994; **91**, 552-63.
[16] JM Bracci, AM Reinhorn and JB Mander. Seismic resistance of reinforced concrete frame structures designed for gravity loads: Performance of structural system. *ACI Struct. J*. 1995; **92**, 597-609.
[17] S Hakuto, R Park and H Tanaka. Seismic load tests on interior and exterior beam-column joints with substandard reinforcing details. *ACI Struct. J*. 2000; **97**, 11-25.
[18] C Liu. 2006, Seismic behaviour of beam-column joint subassemblies reinforced with steel fibers. Master Thesis. University of Canterbury, Christchurch, New Zealand.
[19] MT Tran. Influence factors for the shear strength of exterior and interior reinforced concrete beam-column joints. *Proc. Eng.* 2016; **142**, 63-70.
[20] O Joh, Y Goto and T Shibata. Influence of transverse joint and beam reinforcement and relocation of plastic hinge region on beam column joint stiffness deterioration. *ACI Struct. J*. 1991; **123**, 187-224.
[21] T Kamimura, S Takeda and M Tochio. Influence of joint reinforcement on strength and deformation of interior beam-column subassemblages. *In*: Proceedings of the 12th World Conference on Earthquake Engineering, Auckland, New Zealand. 2000.

[22] S Alavi-Dehkordi, D Mostofinejad and P Alaee. Effects of high-strength reinforcing bars and concrete on seismic behavior of RC beam-column joints. *Eng. Struct.* 2019; **183**, 702-19.
[23] THK Kang, S Kim, JH Shin and JM Lafave. Seismic behavior of exterior beam-column connections with high-strength materials and steel fibers. *ACI Struct. J*. 2019; **116**, 31-43.
[24] SJ Hwang and HJ Lee. Analytical model for predicting shear strengths of exterior reinforced concrete beam-column joints for seismic resistance. *ACI Struct. J*. 1999; **96**, 846-58.
[25] SJ Hwang, HJ Lee, TF Liao, KC Wang and HH Tsai. Role of hoops on shear strength of reinforced concrete beam-column joints. *ACI Struct. J*. 2005; **102**, 445-53.
[26] SJ Hwang, RJ Tsai, WK Lam and JP Moehle. Simplification of softened strut-and-tie model for strength prediction of discontinuity regions. *ACI Struct. J*. 2017; **114**, 1239-48.
[27] ACI Committee 374. *Acceptance criteria for moment frames based on structural testing*. American Concrete Institute, Michigan, 2001.
[28] RL Mayes and RW Clough. *State of the art in seismic shear strength of masonry-an evaluation and review*. EERC Report, California, 1975.
[29] MR Ehsani and JK Wight. Exterior reinforced concrete beam-to-column connections subjected to earthquake-type loading. *ACI Struct. J.* 1985; **82**, 492-9.
[30] G MacGregor and JK Wight. *Reinforced concrete: mechanics and design*. Prentice Hall, New Jersey. 1997.